








Unravelling the atmospheric dynamics involved in flash drought development over Spain

Iván Noguera¹  | Fernando Domínguez-Castro²  |
Sergio M. Vicente-Serrano²  | Ricardo García-Herrera^{3,4}  |
José M. Garrido-Pérez³  | Ricardo M. Trigo⁵  | Pedro M. Sousa^{5,6} 

¹UK Centre for Ecology & Hydrology (UKCEH), Wallingford, UK

²Instituto Pirenaico de Ecología, Consejo Superior de Investigaciones Científicas (IPE-CSIC), Zaragoza, Spain

³Departamento de Física de la Tierra y Astrofísica, Facultad de Ciencias Físicas, Universidad Complutense de Madrid, Madrid, Spain

⁴Instituto de Geociencias (CSIC-UCM), Madrid, Spain

⁵Instituto Dom Luiz (IDL), Faculdade de Ciências, Universidade de Lisboa, Lisbon, Portugal

⁶Instituto Português do Mar e da Atmosfera (IPMA), Lisbon, Portugal

Correspondence

Iván Noguera, UK Centre for Ecology & Hydrology, Maclean Building, Benson Lane, Crowmarsh Gifford, Wallingford, Oxon OX10 8BB, UK.

Email: ivanog@ceh.ac.uk

Funding information

Spanish Ministry of Science, Innovation and Universities, Grant/Award Numbers: TED2021-129152B-C41, PID2020-116860RB-C22, PID2022-218137244OB-I00

Abstract

Flash droughts (FDs) are distinguished by a rapid development associated with strong precipitation deficits and/or increases in atmospheric evaporative demand in the short-term, but little is known about the atmospheric conditions underlying these events. In this study, we analyse for the first time the atmospheric dynamics involved in the development of FDs in Spain over the period 1961–2018. FDs are related to large-scale atmospheric circulation patterns affecting the region, in particular with the positive phase of the North Atlantic Oscillation (NAO). The NAO is the main atmospheric driver of FDs in winter and autumn, and it is essential in explaining FD development in spring. We also found that FDs are typically linked to strong positive anomalies in 500 hPa geopotential height and sea level pressure over the region during the weeks prior to the onset. At the synoptic scale, the most common weather types (WTs) recorded during the development of FDs are Anticyclonic Western (ANT_W_AD), East (E_AD) and Northeast (NE_AD) advection, and Anticyclonic (ANTICYC). In particular, ANTICYC WT is the main atmospheric driver of FDs in summer. Ridging conditions occur frequently during FDs in all seasons, being the most important factor controlling FD development in spring. Likewise, we noted that some of the FDs recorded in summer are related to and/or exacerbated by Saharan air intrusions associated with pronounced ridges. The results of this research have important implications for the understanding, monitoring and prediction of FDs in Spain, providing a detailed assessment of the main atmospheric dynamics involved in FD triggering at different spatial scales.

KEYWORDS

large-scale atmospheric circulation patterns, NAO, ridges and blocks, Saharan intrusions, weather types

This is an open access article under the terms of the [Creative Commons Attribution](https://creativecommons.org/licenses/by/4.0/) License, which permits use, distribution and reproduction in any medium, provided the original work is properly cited.

© 2024 The Authors. *International Journal of Climatology* published by John Wiley & Sons Ltd on behalf of Royal Meteorological Society.

1 | INTRODUCTION

Drought is one of the most damaging natural hazards, and it is characterized by complex and diverse environmental and socioeconomic impacts (Wilhite, 2000; Wilhite & Pulwarty, 2017). Although drought is commonly thought of as a phenomenon that spreads slowly over time and space, its triggering can last from a few weeks to several months. Recently, the term “flash drought” (Svoboda et al., 2002) has become popular to distinguish drought events characterized by rapid development and intensification (Lisonbee et al., 2021). These drought episodes are typically related to anomalous precipitation deficits and/or increases in atmospheric evaporative demand (AED) associated with summer heat waves, which trigger rapid soil moisture depletion and vegetation stress, leading to severe agricultural and environmental impacts within a few weeks (Otkin et al., 2018).

Important efforts have been made in recent years to characterize flash droughts (FDs) in different regions of the world using multiple metrics and methodological approaches (Christian et al., 2019; Mo & Lettenmaier, 2015, 2016; Nguyen et al., 2019; Noguera et al., 2020; Wang et al., 2016; Yuan et al., 2018, 2019). However, some important issues have received little attention, especially those related to the atmospheric dynamics that favour FD onset. While some studies have examined the atmospheric conditions during the occurrence of specific FDs (Liang & Yuan, 2021; Wang & Yuan, 2021; Yuan et al., 2018; Zhang et al., 2017b), few have analysed in detail the atmospheric patterns linked to the occurrence of these events. Focusing exclusively on the patterns in the mid-troposphere, Ford and Labosier (2017) and Mo and Lettenmaier (2016) found that FDs are typically related to a predominance of positive anomalies in geopotential heights at 500 hPa (Z500) over the United States. Mishra et al. (2021) also found positive anomalies in Z500 and sea level pressure (SLP) during FD development over India. In contrast, Wang and Yuan (2018) found no relevant anomalies in Z500 over China, underlining the difficulty of associating this type of event with a specific synoptic configuration in this region.

In Spain, drought occurrence responds to a wide variety of atmospheric dynamics operating at different spatial scales. Numerous studies have demonstrated the influence of the frequency of daily weather types (WTs) on precipitation (Cortesi et al., 2014; Goodess & Jones, 2002; Paredes et al., 2006; Trigo & DaCamara, 2000) and air temperature (Fernández-Montes et al., 2013; García et al., 2002; García-Herrera et al., 2005; Peña-Angulo et al., 2016). Likewise, the relationship between these

synoptic situations and the occurrence of droughts has been investigated (Russo et al., 2015; Vicente-Serrano & López-Moreno, 2006). For example, Olcina-Cantos (2001) described the persistence of anticyclonic and high-pressure systems as the usual situations underlying the occurrence of drought in Spain. Other authors have examined the particular synoptic situations involved in the development of some extreme drought events in both cold and warm periods (García-Herrera et al., 2007; Serrano-Notivoli et al., 2023), demonstrating the complex atmospheric dynamics controlling drought occurrence in Spain.

Several studies have also shown the relationship between large-scale atmospheric circulation patterns and drought severity in Spain at the monthly/seasonal scale (Manzano et al., 2019; Vicente-Serrano & López-Moreno, 2006). In this regard, the North Atlantic Oscillation (NAO) is widely considered as the main atmospheric mechanism controlling precipitation in Spain (Martín Vide & Fernández, 2001; Rodríguez-Puebla et al., 1998; Trigo et al., 2004), and its influence on droughts in the Iberian Peninsula is well known (Manzano et al., 2019; Trigo et al., 2013; Vicente-Serrano et al., 2011; Vicente-Serrano & López-Moreno, 2006). In addition, other regional atmospheric circulation mechanisms such as the Mediterranean Oscillation (MO) (Conte et al., 1989) and the Western Mediterranean Oscillation (WeMO) (Martín-Vide & Lopez-Bustins, 2006) also play a relevant role in precipitation variability over Mediterranean regions (Düneloh & Jacobeit, 2003; Rodríguez-Puebla et al., 2001) and, consequently, in the occurrence of droughts. Some authors have evidenced the link between these large-scale atmospheric circulation patterns (i.e., NAO, MO, WeMO) and air temperature over the Iberian Peninsula and Mediterranean regions (Castro-Díez et al., 2002; El Kenawy et al., 2012; Rodríguez-Puebla et al., 2010; Sáenz et al., 2001a, 2001b; Xoplaki et al., 2003), which could have a certain role in triggering drought conditions in the warm season.

Spain is also affected by other specific atmospheric configurations and mechanisms that can trigger drought conditions. The presence of ridge and blocking structures over the Iberian Peninsula or in its close vicinity can play a crucial role in causing both precipitation deficits and notable AED increases in Spain related, for example, to heat wave episodes (Ionita et al., 2017; Serrano-Notivoli et al., 2022; Sousa et al., 2016, 2018). In particular, the occurrence of Saharan air intrusions, frequently associated with pronounced ridges that promote additional solar heating under clear skies, as well as warm horizontal advection and vertical downward air mass movements that further warm the surface, have an important role in promoting heat waves in the Iberian Peninsula in

summer (Sousa et al., 2019). Thus, Saharan air intrusions may be a relevant atmospheric mechanism for triggering and/or exacerbating FDs associated with extreme temperature episodes during the summer months in Spain. Although FDs in Spain are mainly driven by precipitation variability, the role of AED is essential to explain the development of FDs over southern and southeastern regions during the warm season (Noguera et al., 2022). Therefore, these mechanisms could have important implications for the triggering of this type of event in Spain.

In summary, we can state that several studies have analysed the variety of atmospheric conditions involved in the occurrence of drought episodes in Spain (Vicente-Serrano, 2021), but there is a gap in the knowledge of the atmospheric dynamics associated with FDs. Although the complex atmospheric dynamics driving drought variability in Spain have been studied (Manzano et al., 2019; Olcina-Cantos, 2001), their role in the occurrence of FDs is poorly understood. Consequently, we present the first characterization of the atmospheric dynamics involved in the development of FDs in Spain. With this aim we will (i) evaluate the influence of some of the main large-scale atmospheric circulation patterns in Spain (i.e., NAO, MO and WeMO) on FD onset, (ii) analyse the atmospheric configurations at the synoptic scale (WTs) associated with FDs, (iii) investigate the possible role of ridge and blocking structures as well as Saharan air intrusions in triggering FDs, and finally (iv) determine which of these atmospheric drivers are the most relevant in the development of FDs.

2 | DATA AND METHODS

2.1 | Meteorological data

We used a high spatial resolution (1.21 km²) gridded dataset of meteorological data for mainland Spain and the Balearic Islands for the period 1961–2018. This dataset includes weekly data on precipitation, maximum and minimum air temperature, relative humidity, sunshine duration and wind speed, and was generated using all available daily observations from the National Spanish Meteorological Service (AEMET). The observations were subjected to a thorough quality control (Tomás-Burguera et al., 2016). Details on the construction and validation of the dataset can be found in Vicente-Serrano et al. (2017). The FAO-56 Penman–Monteith equation (Allen et al., 1998) was used to calculate the AED from the gridded data of air temperature, relative humidity, wind speed and sunshine duration.

2.2 | Flash drought identification and development phase

We identified FDs using the Standardized Precipitation Evapotranspiration Index (SPEI) (Vicente-Serrano et al., 2010), one of the most widely used drought indices worldwide (Mukherjee et al., 2018). It is calculated in a similar way to the Standardized Precipitation Index (SPI), but the SPEI is based on the climatic water balance rather than on precipitation. The climatic water balance compares the water available (i.e., precipitation) with the atmospheric evaporative demand (AED). This difference between precipitation and AED is calculated at different time scales (e.g., 1, 3, 6, 12 months) and fitted to a log-logistic probability distribution to obtain standardized units that are comparable over the time and space (Beguería et al., 2014). By including the role of the AED, the SPEI can capture the effect of rising temperatures on drought severity, which is essential for a reliable drought assessment in the current global warming context (Cook et al., 2014). Thus, the SPEI is sensitive to precipitation variability, but also to increases in AED, especially during dry and warm periods when AED is more important in triggering drought (Tomás-Burguera et al., 2020). Numerous studies have used the SPEI to analyse the response of hydrological (McEvoy et al., 2012; Peña-Gallardo et al., 2019a; Vicente-Serrano & López-Moreno, 2005; Zhang et al., 2015), agricultural (Peña-Gallardo et al., 2019b; Potop et al., 2012; Potopová et al., 2016) and environmental (Caminero et al., 2018; Vicente-Serrano et al., 2013; Xu et al., 2018; Zhang et al., 2017a) systems to drought. Previous studies have also demonstrated the good performance of SPEI in identifying and quantifying FDs under different climatic conditions (Hunter et al., 2014; Noguera et al., 2020, 2021).

Following Noguera et al. (2020), we employed the SPEI at a short time scale (1 month) and weekly frequency to identify rapid and strong changes in SPEI that are characteristic of a FD onset (Otkin et al., 2018; Svoboda et al., 2002). In order to be considered a FD, a candidate event must fulfil several conditions, namely: (i) a minimum length of 4 weeks in the development phase; (ii) a decline in SPEI equal to or less than 2 z-units; and (iii) a final SPEI value equal to or less than -1.28 z-units (corresponding to return periods of 10 years). Further details of the method used to identify FD events are available in Noguera et al. (2020), which also provides a full characterization of the seasonal spatial pattern of FDs in Spain, as well as the temporal evolution of these phenomena over the last six decades.

To analyse the atmospheric dynamics involved in the development of FDs in Spain, we focused on the atmospheric conditions recorded during the 4 weeks prior to

the onset (i.e., the development phase according to Noguera et al., 2020). This 4-week temporal lapse established for the development phase of the FDs agrees with some of the most widely used definitions for the assessment of FDs (Anderson et al., 2013; Chen et al., 2019; Christian et al., 2019; Mukherjee & Mishra, 2022; Osman et al., 2021), as it allows to capture rapid variations in humidity conditions but persisting long enough to have an impact. By focusing on the development phase, we could determine the atmospheric conditions driving the rapid declines in SPEI values associated with short-term anomalies in precipitation and AED that trigger FDs. We conducted our analysis on the events with the largest affected area in each season over the domain of study in order to capture representative seasonal characteristics of FDs for the whole of Spain. Thus, we selected the top-10 FDs identified in each season (winter: DJF, spring: MAM, summer: JJA and autumn: SON) for the period 1961–2018 according to the percentage of the area of mainland Spain and Balearic Islands area affected in a given week.

2.3 | Atmospheric data

We used several sources of atmospheric information. First, we obtained daily SLP and Z500 data from the National Centers for Environmental Prediction (NCEP)–National Center for Atmospheric Research (NCAR) (<https://psl.noaa.gov/data/>) for the domain study area (25°–70°N, 30°W–30°E) over the period 1961–2018 at 5° spatial resolution. We then computed weekly anomalies in SLP and Z500 over the development phase of each of the top-10 FDs identified in each season. The anomalies are relative to the average SLP and Z500 recorded for the period 1961–2018.

SLP data from NCEP–NCAR reanalysis were used to compute three large-scale atmospheric circulation indices, namely the North Atlantic Oscillation (NAO), the Mediterranean Oscillation (MO) and the Western Mediterranean Oscillation (WeMO). We calculated the NAO index (NAOi) following the classical approach of Jones et al. (1997), which is based on the differences between normalized SLP at the points 36°N, 5°W (Gibraltar, UK) and 65°N, 20°W (Reykjavik, Iceland). The MO index (MOi) was originally defined as the difference of standardized SLP at the point 36.4°N, 3.1°E (Algiers, Argel) and 30.1°N, 31.4°E (Cairo, Egypt) by Conte et al. (1989), but in this case we adopted the method proposed by Palutikof (2003), which is based on the differences between normalized SLP at the points 36°N, 5°W (Gibraltar, UK) and 31°N, 34°E (Lod, Israel). Finally, to compute the WeMO index (WeMOi), we adopted the original

approach proposed by Martin-Vide and Lopez-Bustins (2006) based on the difference between normalized SLP at the points 36°N, 6°W (San Fernando, Spain; in this case extended from Gibraltar due to its proximity) and 45°N, 11°E (Padua, Italy). We then calculated the average anomalies recorded for each index over the development phase of each of the top-10 FDs identified in each season between 1961 and 2018.

Using SLP and Z500 data, we also applied a daily WT classification by means of an improved Jenkinson and Colison (1977) approach, which allows for the consideration of atmospheric conditions at both surface and mid-troposphere (see details in Miró et al., 2020). The method classifies daily WTs into 15 categories: West advection (W_AD), Anticyclone West advection (ANT_W_AD), Northwest advection (NW_AD), North advection (N_AD), Northeast advection (NE_AD), East advection (E_AD), East Advection with cut-off above (E_AD_CUT), South advection (S_AD), Southwest advection (SW_AD), Trough (TROUGH), Cyclone (CYCLONIC), Thermal low (THERMAL_L), Anticyclonic (ANTICYC), Thermal anticyclone (THERMAL_ANTIC) and Shallow Cyclone (SHA). Figures S1 and S2 show the composites of the average Z500 and SLP conditions associated with each WT. The percentage of days under each one of the WTs was summarized over the development phase of each of the top-10 FDs identified in each season. In addition, we calculated the seasonal frequency anomalies for each WT (expressed as % of days) compared to the climatological average of these WTs for the period 1961–2018.

We assessed the role of ridge and blocking structures employing a recently developed dataset that contains a complete catalogue of all ridges and blocks that occurred over the Iberian Peninsula. This catalogue includes the ridge and blocking (classified into Omega, Rex hybrid and Rex pure) structures recorded at daily scale (see details in Sousa et al., 2021). We considered those ridges and blocks recorded between the latitudes 30°–45°N and between the longitudes 20°W–10°E for the period 1961–2018. The percentage of days under each of these structures (i.e., ridge, omega block, rex hybrid block and rex pure block) was summarized over the development phase of each of the top-10 FDs identified in each season. In addition, we calculated the seasonal frequency anomalies of each structure (expressed as % of days) compared with the climatology average of these structures for the period 1961–2018.

Finally, to specifically examine the possible role of Saharan intrusions in summer FDs, we used a daily dataset that records all Saharan air intrusion episodes affecting the Iberian Peninsula for the period 1961–2018 (see details in Sousa et al., 2019). We considered as Saharan air intrusion conditions those days when air masses with

desertic characteristics (i.e., very hot and dry) originating from Africa were recorded north of 35°N and between the longitudes 10°W–5°E. The percentage of days under Saharan air intrusions was summarized over the development phase of each of the top-10 FDs identified in summer. In addition, we calculated the frequency anomalies in Saharan air intrusions (expressed as % of days) compared with the climatology average of Saharan air intrusions in summer for the period 1961–2018.

2.4 | Stepwise logistic regression

To determine which atmospheric drivers are most relevant in explaining FDs, we applied a stepwise logistic regression model based on a forward selection. The logistic regression model is an advantageous technique to examine the possible relationship between a dependent variable or response (i.e., the presence or absence of FD development conditions) and different independent variables or predictors (i.e., anomalies in NAOi, MOi and WeMOi, days (%) under each WT, days (%) under each ridge and blocking structure and days (%) under Saharan air intrusions) (Hosmer et al., 1989; Peng et al., 2002). We used a stepwise forward procedure to select the most relevant predictors in explaining the occurrence of a response (i.e., the most important atmospheric drivers to explain FD development) according to statistical criteria (Desboulets, 2018). Thus, the model starts with no variables, and progressively adds the predictors that most improve the fit, until the inclusion of new ones no longer improves the model. The model was run using the StepAIC function, based on the Akaike information criterion (AIC) (Akaike, 1974), as it makes possible to automate the stepwise forward selection process and remove the possible multicollinearity of the predictors (Venables & Ripley, 2002). We focused on the development weeks of the top-10 FDs identified in each season to unravel which variables are most relevant in triggering flash droughts. The stepwise logistic regression analysis provides information on both the significance (p -values) and relevance (z -standardized coefficients) of each predictor selected for the model. The results shown include only those predictors with a $p < 0.05$ (95% of confidence interval) for each season.

3 | RESULTS

3.1 | Diversity of atmospheric dynamics underlying FDs in Spain

To illustrate the wide variety of atmospheric dynamics that can be involved in the development of FDs

seasonally, events with different characteristics are shown in Figures 1 and 2. Thus, we selected FDs occurred during cold periods that were mainly associated with strong precipitation anomalies (i.e., 1962 and 1997 FDs), as well as FDs occurred during warm periods that were closely related to remarkable anomalies in AED (i.e., 1978 and 2015 FDs).

In general, important variations were observed between the atmospheric configurations prior to the onset of FDs in cold (Figure 1) and warm (Figure 2) seasons, as well as in the atmospheric mechanisms driving their onset (Table 1). For example, the synoptic configuration preceding the Feb 1962 FD showed the predominance of patterns typically associated with strong precipitation deficits over Spain during winter (Figure 1a), namely NE_AD and ANTICYC WTs (Table 1). These preceding weeks reveal a relatively stable pattern characterized by a very high-pressure system over the Iberian Peninsula and a dominant omega block structure, resulting in strong precipitation deficits over Spain. The large-scale NAO pattern was in a positive phase in the weeks preceding the onset of the FD, with anomalies around one z -unit in the NAOi. Similarly, positive anomalies were recorded in the MOi during these weeks. The synoptic configuration during the development weeks leading to Feb 1997 FD also exhibited omega and rex hybrid patterns usually linked to the absence of precipitation over Spain in winter and autumn (Figure 1b). Blocking patterns were frequent during these weeks (including Omega and Rex types). Unlike the Feb 1962 event, the dominant synoptic patterns in this case were the ANT_W_AD, followed by ANTICYC WT (Table 1). This event was strongly driven by a positive NAO (3.24 z -units) and the presence of very anomalous high-pressure systems affecting southern Europe.

In summer, the atmospheric dynamics that trigger FDs vary considerably, with important differences even between FD events (Figure 2). The development of the Aug 1978 FD showed a pattern related to a heat wave that affected Spain in mid-July (Figure 2a), with a dominance of NE_AD and N_AD WTs (Table 1). A high-pressure system was observed at sea level during the weeks preceding the onset of the FD, while the mid-troposphere pattern at Z500 varied considerably, with some days under Saharan air intrusions (~23%) associated with the dominance of ridging conditions during these weeks. Different atmospheric patterns were observed during the weeks previous to the Jul 2015 FD (Figure 2b); recording anticyclonic conditions (E_AD, NE_AD and ANT_W_AD) over the Iberian Peninsula, which resulted in a heat wave in July with several episodes of extreme temperatures that caused a dramatic decrease in humidity. This event was also closely related

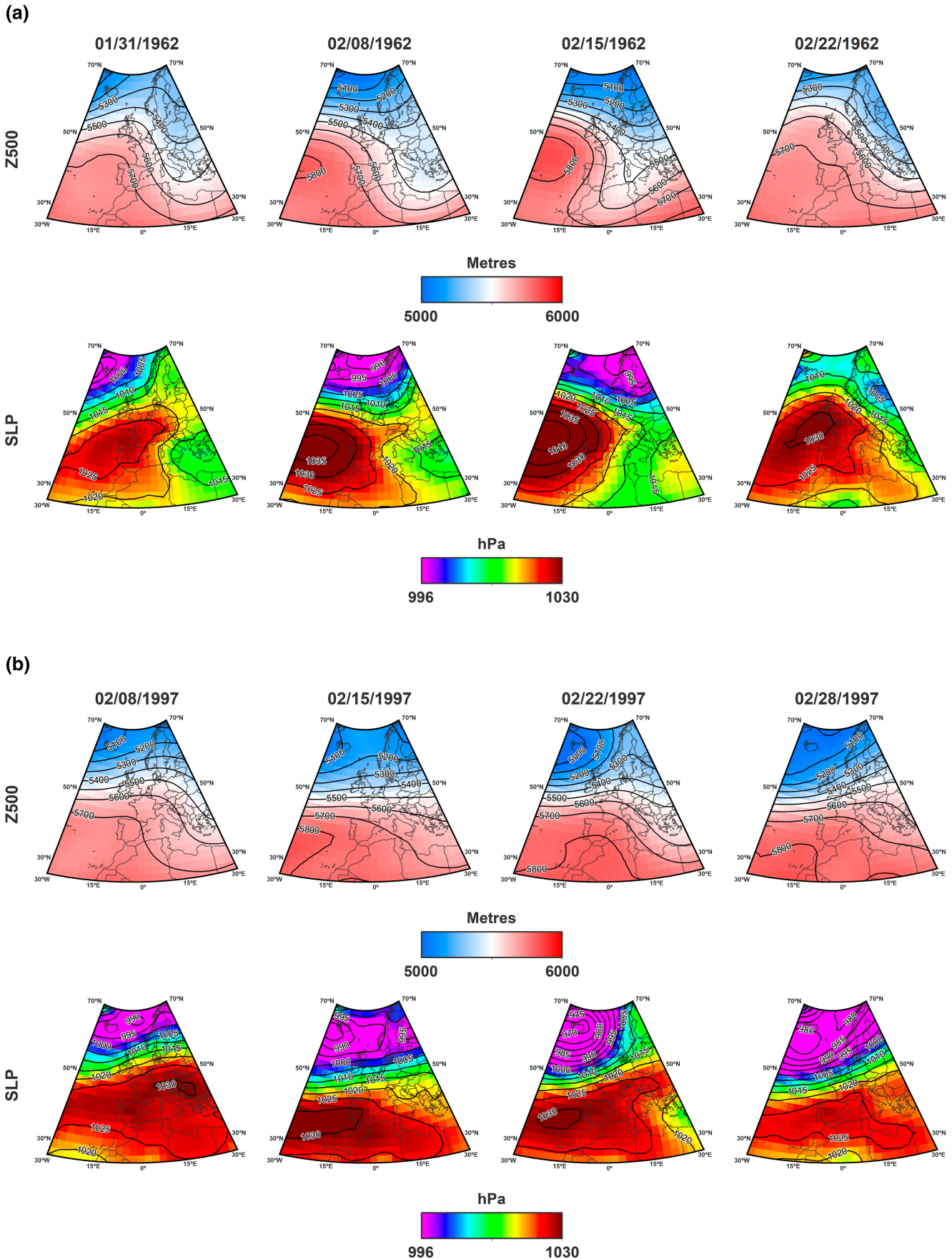


FIGURE 1 Weekly composites of the average Z500 (metres) and SLP (hPa) during the development of the winter (a) Feb 1962 and (b) Feb 1997 FDs.

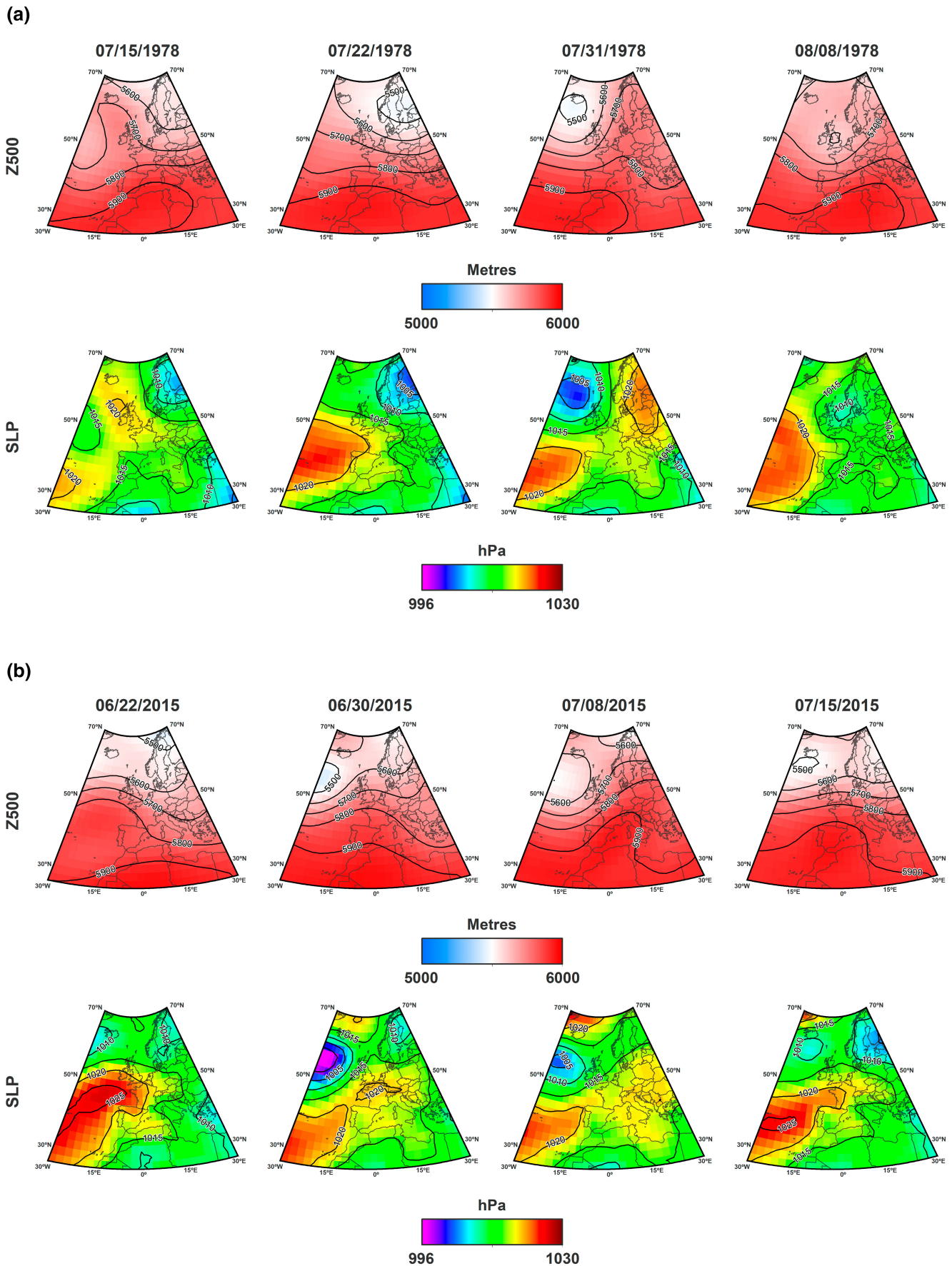


FIGURE 2 Weekly composites of the average Z500 (metres) and SLP (hPa) during the development of the summer (a) Aug 1978 and (b) Jul 2015 FDs.

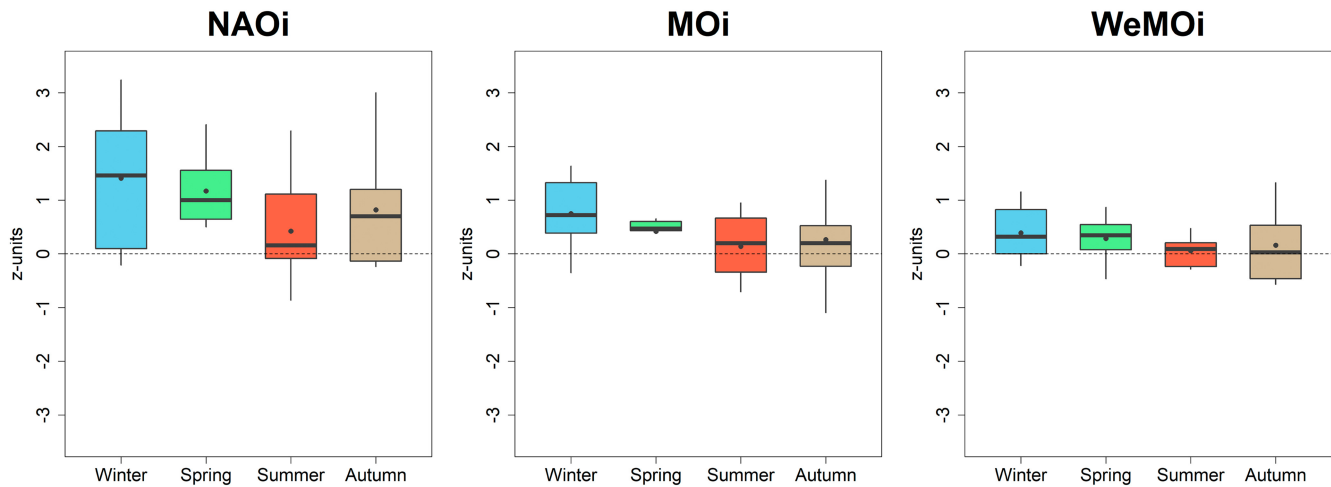


FIGURE 3 Average anomalies in North Atlantic Oscillation index (NAOi), Mediterranean Oscillation index (MOi) and Western Mediterranean Oscillation index (WeMOi) during the development phase of the top-10 FDs for each season over the period 1961–2018. The box represent the 1st and 3rd quartiles, while the brackets show the maximum and minimum values. Horizontal lines in the boxplot represent the median and the points represent the average.

to Saharan air intrusions (~57% of the days during the event) associated with pronounced ridge conditions in the mid-troposphere (Table 1). These four examples illustrate the diversity of the atmospheric drivers that can trigger FD conditions in Spain seasonally.

3.2 | Relationship between the atmospheric dynamics and FDs development

The development of the top-10 FDs in Spain exhibits a close relationship with the large-scale atmospheric circulation patterns affecting Spain (Figure 3). In general, the triggering of FDs corresponds to periods of positive anomalies in NAOi, although the average amplitude of these anomalies varies notably among seasons. The largest anomalies in NAOi are found in winter, with average values around 1.5 z-units during the development of the recorded top-10 FDs. Strong anomalies in the NAOi were also found during the triggering of FDs in spring and autumn, with average values of ~1.2 and ~0.8 z-units, respectively. Positive anomalies were also recorded in MOi during the development of the top-10 FDs in all seasons. The strongest MOi anomalies during the triggering of the FDs occur in winter and spring, with average values around 0.7 and 0.5 z-units, respectively. The WeMOi anomalies during the periods of FD development were small and close to zero in all seasons, suggesting a lower influence on the FD onset compared to the NAOi and the MOi.

In Spain, FD development is typically associated with positive SLP and Z500 anomalies centred northwest of

the Iberian Peninsula (Figure 4). These positive anomalies correspond to an Azores High displaced towards northern Iberia associated with an enhanced ridge in the mid-troposphere, both features inhibiting the usual West–East movement of mid-latitude low-pressure systems. These conditions are observed during the previous weeks to the onset of FDs in all seasons, albeit with considerable stronger signal in winter (for both SLP and Z500) than in summer (Figure 4).

Table 2 shows the percentage of days under each WT category during the development of the top-10 FDs in each season, as well as the corresponding frequency anomalies. In general, ANT_W_AD and E_AD were the most frequent WTs during the development of the FDs in Spain, with more than 19% of the days regardless of the season; while THERMAL_L, THERMAL_ANTIC, TROUGH, CYCLONIC and SHA were the least frequent, with percentages less than 1%. In winter, ANT_W_AD, E_AD, ANTICYC and NE_AD WTs recorded important positive frequency anomalies. Likewise, spring FDs were characterized by unusually high frequencies of ANT_W_AD, E_AD, NE_AD and ANTICYC WTs in comparison with the climatological frequency of these WTs. The smallest frequency anomalies were found in summer, being ANT_W_AD and ANTICYC those that show the largest positive anomalies. Finally, the highest positive frequencies of WTs associated with FDs in comparison to the autumn climatology were E_AD, ANT_W_AD, NE_AD and ANTICYC. Therefore, we can summarize that the following four WTs: ANT_W_AD, E_AD, NE_AD and ANTICYC were generally the most frequent during the development of FDs. It is also important to stress that several WTs present consistent negative

TABLE 1 Average anomalies in large-scale circulation indices (NAOi, MOi and WeMOi) and percentage of days under each WT, ridge and block structure (RIDGE, OMEGA and REX HYBRID) and Saharan intrusions (SAHARAN_INT) during the development (i.e., 4 weeks prior to the onset) of 1962, 1978, 1997 and 2015 FDs.

Flash droughts	Feb 1962	Aug 1978	Feb 1997	Jul 2015
NAOi	1.03	-0.08	3.24	0.23
MOi	1.39	0.73	0.49	-0.19
WeMOi	0.48	0.21	0.82	-0.28
RIDGE	19.36	25.81	57.14	70.00
OMEGA	85.71	37.50	33.33	0.00
REX HYBRID	0.00	0.00	33.33	0.00
SAHARAN_INT	0.00	22.58	0.00	56.66
W_AD	0.00	0.00	7.14	6.66
ANT_W_AD	6.45	16.13	50.00	13.33
NW_AD	3.23	0.00	0.00	10.00
N_AD	6.45	35.48	0.00	3.33
NE_AD	38.70	41.94	7.14	26.66
E_AD	0.00	6.45	10.71	30.00
E_AD_CUT	0.00	0.00	0.00	3.33
ANTICYC	19.35	0.00	25.00	6.66
SHA	3.25	0.00	0.00	0.00

Note: We have excluded from this table the WTs and block structures that did not occur during any of the four events.

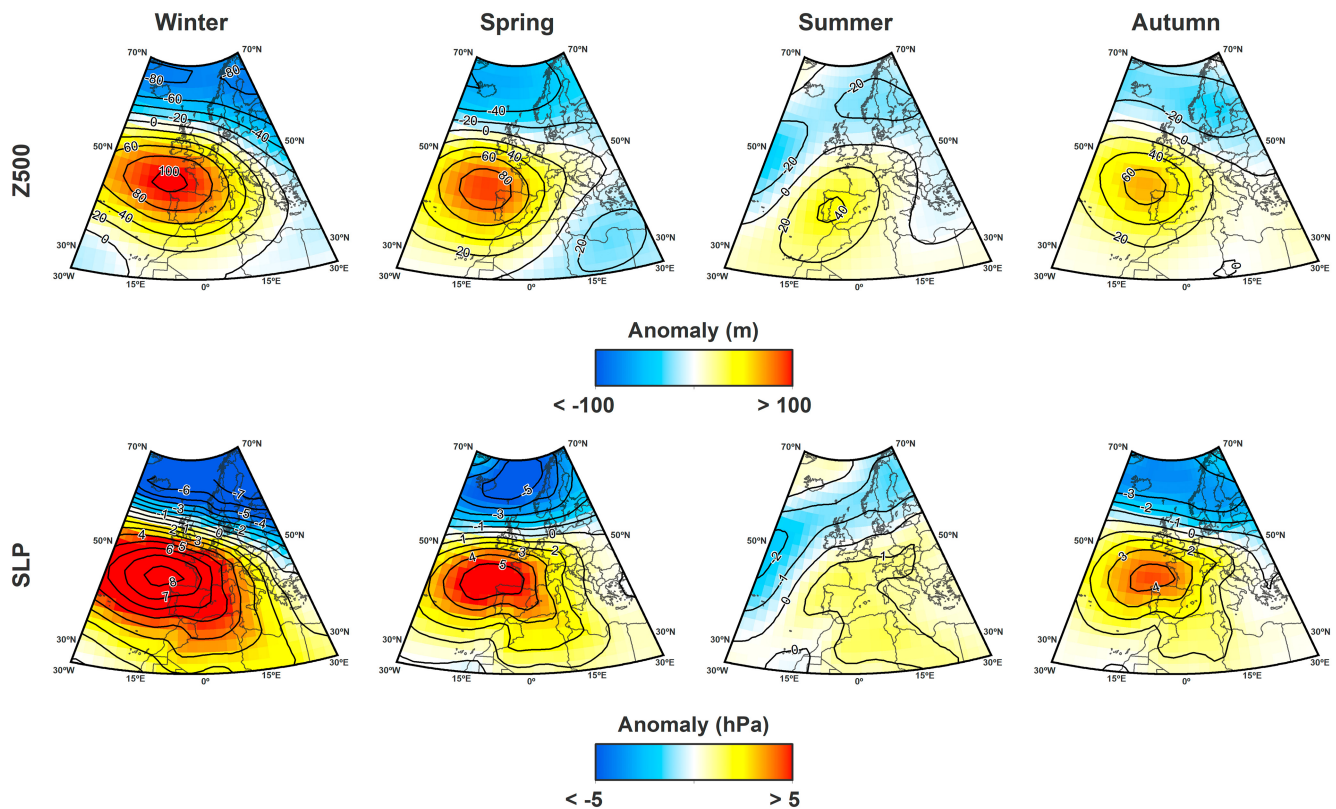


FIGURE 4 Composite of the anomalies in Z500 (metres) and SLP (hPa) during the development of the top-10 FDs in each season over the period 1961–2018.

TABLE 2 Percentage of days under each WT during the development of the top-10 FDs and frequency anomalies (%) recorded in each season over the period 1961–2018.

	Winter		Spring		Summer		Autumn	
	FDs	Anomalies	FDs	Anomalies	FDs	Anomalies	FDs	Anomalies
W_AD	3.69	−7.77	1.99	−6.22	3.56	1.09	2.97	−4.99
ANT_W_AD	28.19	11.47	23.92	8.25	24.92	7.38	24.42	6.46
NW_AD	4.70	−5.12	5.32	−5.39	7.12	−1.14	4.29	−4.69
N_AD	6.38	−1.17	10.30	−1.30	14.56	−1.54	7.92	−0.72
NE_AD	12.08	4.53	17.61	6.01	18.12	−4.70	13.53	4.30
E_AD	19.46	6.43	23.92	6.51	23.95	0.99	27.06	8.23
E_AD_CUT	2.68	−1.08	1.66	−1.26	1.29	−0.15	3.63	0.43
S_AD	3.36	−0.37	3.32	0.68	0.65	−0.01	2.64	−1.36
SW_AD	1.68	−6.21	1.66	−2.93	0.97	0.31	2.31	−4.91
TROUGH	0.00	−0.97	0.00	−0.86	0.65	0.18	0.33	−0.54
CYCLONIC	0.34	−4.19	0.33	−5.78	0.00	−1.84	0.66	−4.04
THERMAL_L	0.00	0.00	0.00	−1.29	0.65	−3.44	0.00	−1.21
ANTICYC	16.78	6.25	9.30	5.22	3.56	2.87	8.91	3.23
THERMAL_ANTIC	0.34	0.09	0.00	−0.22	0.00	0.00	0.33	0.18
SHA	0.34	−1.88	0.66	−1.42	0.00	0.00	0.99	−0.37

Note: Bold indicates the most remarkable positive and negative frequencies anomalies at each season.

frequency anomalies during the top-10 FDs. This is clearly the case of three WTs that are often associated with higher than usual precipitation over Spain in winter, spring and autumn: W_AD, NW_AD and CYCLONIC.

Table 3 shows the percentage of days with the presence of different synoptic structures (i.e., ridge, omega block, rex hybrid block, rex pure block) around the Iberian Peninsula during the development of the FDs in each season, as well as the frequency anomalies in comparison with the climatological frequency of these structures. Overall, the ridge and omega block are the most frequent structures during FD triggering in every season. In winter, omega block and ridge structures are the most frequent, with very noticeable positive frequency anomalies in omega blocks compared to the average climatology. Spring FDs are characterized by a high percentage of days under ridge and omega structures, with positive frequency anomalies above 6%. In summer, ridges are the most frequent structures during the development stages of the top-10 FDs. However, these patterns are so prevalent during the summer months that FD frequency anomalies are neglectable. Omega blocking is also relatively frequent (~24%), but this percentage is smaller in comparison with the climatology. In autumn, while blocking structures show frequencies close to the average climatology, ridges are associated with frequency anomalies above 9%, illustrating its relationship with FDs occurrence.

We also found that some of the FDs recorded in summer developed during episodes of Saharan air intrusion. Nevertheless, there are no relevant differences between the Saharan intrusion conditions reported during FDs triggering (11%) and the climatology (11.7%). It is noteworthy, however, that the development of 4 of the top-10 FDs recorded in summer was characterized by the occurrence of Saharan intrusion conditions, and in 3 of them these conditions were recorded on at least 22% of the FD development days (e.g., Figure 2).

3.3 | Key atmospheric dynamics explaining FDs development

After assessing the relationship between FDs and different atmospheric dynamics, we employ a stepwise procedure to select the optimal set of predictors (i.e., atmospheric drivers) using a logistic regression model. Table 4 shows the standardized coefficients and p-values of the model predictors that significantly explain the development of the top-10 FDs identified in each season over the period 1961–2018. The NAO is the main driver to explain FDs triggering in winter, with a strong relationship between positive anomalies in NAOi and the development of FDs. Besides, there is a close relationship between a low percentage of days under W_AD and SW_AD WTs and FD triggering in winter, which shows a

TABLE 3 Percentage of days under each ridge and blocking structure (ridge, omega block, rex hybrid block, rex pure block) during the development of the top-10 FDs and frequency anomalies (%) recorded in each season over the period 1961–2018.

	Winter		Spring		Summer		Autumn	
	FDs	Anomalies	FDs	Anomalies	FDs	Anomalies	FDs	Anomalies
Ridge	42.33	2.96	58.18	6.10	52.62	−2.28	54.12	9.81
Omega	45.91	20.80	34.37	6.87	23.56	−6.89	23.21	−1.54
Rex Hybrid	9.60	−5.70	13.25	−2.82	5.42	1.44	3.38	−2.44
Rex Pure	1.72	−3.61	3.40	−3.61	1.48	0.52	0.00	−1.66

TABLE 4 Logistic regression standardized coefficients and *p*-values for model parameters that showed a significant relationship (*p*-value <0.05) with the development of the top-10 FDs for each season in the period 1961–2018.

	Winter		Spring		Summer		Autumn	
	Z value	<i>p</i> -value	Z value	<i>p</i> -value	Z value	<i>p</i> -value	Z value	<i>p</i> -value
NAOi	4.19	<0.01	2.00	0.04	-	-	2.50	0.01
RIDGE	-	-	2.22	0.02	-	-	-	-
W_AD	−2.49	0.01	−2.65	<0.01	-	-	-	-
NW_AD	-	-	-	-	-	-	−2.06	0.03
SW_AD	−2.27	0.02	-	-	-	-	−2.22	0.03
ANTICYC	-	-	-	-	2.92	<0.01	-	-
CYCLONIC	-	-	−1.98	0.04	-	-	−2.07	0.04

negative relationship between the occurrence of these WT and FDs. In spring, FDs were mainly related to a high percentage of days with ridging conditions and positive values of the NAOi; moreover, a low percentage of days under W_AD and CYCLONIC WT is also essential in explaining FD onset. In contrast, summer FDs are closely associated with a high percentage of days under ANTICYC WT, which is the main driver of FDs in this season. In autumn, results show again a close link between positive anomalies in NAOi and FD development. Likewise, a low percentage of days under SW_AD, CYCLONIC and NW_AD WT shows a close and negative relationship with the triggering of FDs in autumn.

4 | DISCUSSION

This study has analysed for the first time the atmospheric dynamics associated with the development of FDs in Spain. Despite the efforts made in recent years to characterize FDs in different regions of the world (Christian et al., 2019; Mo & Lettenmaier, 2015, 2016; Nguyen et al., 2019; Noguera et al., 2020; Wang et al., 2016; Yuan et al., 2018, 2019), few studies have focused on the atmospheric conditions underlying the occurrence of FDs (e.g., Ford & Labosier, 2017). To achieve this aim, we

have evaluated the role played by a wide range of atmospheric circulation patterns, including both large (e.g., NAO, blocking structures) and synoptic (e.g., WT) scales, and considering the lower (SLP) and mid-troposphere (Z500) layers. Thus, we demonstrate that diverse atmospheric dynamics can be involved in FD triggering over Spain, with important seasonal contrasts. Among others, we identified certain key atmospheric drivers that are crucial in explaining the development of FDs.

FD development is closely related to NAO patterns. The relationship between positive NAO and low precipitation over the Iberian Peninsula is well known, especially in winter (Rodríguez-Puebla et al., 2001; Trigo et al., 2004), but also during autumn and, to a lesser extent, in spring (Martín Vide & Fernández, 2001). In this way, we found that the NAO is the most important factor for FD development in winter and autumn, but it is also essential for FD triggering in spring. During these seasons, the development of FDs in Spain responds mainly to precipitation deficits (Noguera et al., 2022), so it is reasonable that the NAO plays a key role since it strongly controls precipitation variability over Spain (Esteban-Parra et al., 1998). Similarly, previous studies evidenced the strong influence of the NAO in triggering drought conditions over Iberian Peninsula (Manzano et al., 2019;

Trigo et al., 2013; Vicente-Serrano et al., 2011; Vicente-Serrano & Cuadrat, 2007). Although some studies have also noted a certain link between the occurrence of droughts in some regions of Spain and WeMO and MO patterns (Manzano et al., 2019), we did not find a clear influence of these patterns on FDs. However, it should be noted that the effect of WeMO and MO on precipitation over Spain shows important regional contrast (Martin-Vide & Lopez-Bustins, 2006), so their possible influence could be masked by focusing on FDs events that affected large areas.

At the synoptic scale, FD development in Spain is normally associated with high-pressure systems and atmospheric stability over the Iberian Peninsula. Strong positive anomalies in SLP and Z500 were found in winter, spring and autumn due to strong anticyclones displaced towards northwestern Iberia (see Figure S3), leading to strong precipitation deficits (Muñoz-Díaz & Rodrigo, 2006), which are essential for triggering FDs in these months (Noguera et al., 2022). In summer, when atmospheric stability and low-pressure gradients are dominant over Spain (García-Valero et al., 2012), the climatology is more favourable for FD development and large anomalies in SLP and Z500 are not essential. In general, the percentage of days under WTs associated with anticyclonic situations, such as ANT_W_AD, E_AD, NE_AD and ANTICYC (see Figures S1 and S2), recorded positive anomalies compared to the climatological frequency of these WTs. In particular, ANTICYC WT, which results in atmospheric stability that promotes the absence of precipitation and higher temperatures during the warm season (Martin-Vide & Olcina-Cantos, 2001; Molina, 1981), is the main driver of FDs in summer. On the contrary, WTs commonly associated with atmospheric instability and precipitation such as W_AD, NW_AD, SW_AD, TROUGH, CYCLON and SHA generally recorded negative anomalies during the development of FDs. In fact, some of these WTs exhibit a close and negative relationship with FDs in winter (i.e., W_AD and SW_AD), spring (i.e., W_AD and CYCLONIC) and autumn (i.e., NW_AD, SW_AD and CYCLONIC), which obviously shows that a low percentage of days under these WTs is essential for FDs occurrence.

FDs development is also usually associated with a high percentage of days with a ridge structure in all seasons, which generally leads to precipitation scarcity over Spain as it prevents the arrival of storms in the region (Santos et al., 2009; Sousa et al., 2016, 2018). In particular, anomalous ridging conditions are highly frequent during spring FDs, being the main atmospheric driver of FDs in this season. The anomalies recorded in the frequency of omega blockings in the winter FDs, which usually result in a lack of precipitation (Sousa et al., 2021)

are relevant but are not among the main predictors of FDs in these months. We also found that some of the summer FDs occurred during Saharan air intrusion episodes associated with pronounced ridges that promote the arrival of warm air masses to the Iberian Peninsula (e.g., 2015 FD). Although the advection of these dry and warm air masses from northern Africa contributes to the temperature increase (García-Herrera et al., 2005) and, consequently, favours FD conditions, we did not find any relevant frequency anomalies.

Our findings illustrate the diversity of large-scale atmospheric circulation patterns, synoptic situations and atmospheric mechanisms that may underlie the triggering of FDs. Although the atmospheric conditions that drive FDs could be very variable worldwide, it is expected that these events may be associated with high-pressure systems and atmospheric stability leading to low precipitation, clear skies or increases in AED that drive FD development (Otkin et al., 2018). In this way, the patterns observed prior to the onset of FDs in Spain are very consistent with those found in previous studies over India (Mishra et al., 2021) and the United States (Ford & Labosier, 2017; Mo & Lettenmaier, 2016), which reported positive anomalies at sea level and 500 hPa during the development of FDs. In addition, we noted important seasonal variations in the atmospheric dynamics involved in the triggering of FDs in Spain. The results suggest that the development of FDs occurring during winter, spring and autumn responds mainly to large-scale atmospheric circulation patterns, which control precipitation variability (e.g., NAO). While in the summer, when the precipitation is very low in most of Spain (Serrano et al., 1999), thermodynamic processes associated with atmospheric stability conditions promoting temperature and AED rise seem to be more relevant in explaining FDs. It is expected that these patterns can be extended to other regions in the mid-latitudes where the atmospheric mechanisms driving drought usually show a marked seasonality.

5 | CONCLUSIONS

In this study, we analysed for the first time the atmospheric dynamics involved in the development of FDs in Spain. To achieve this, we examined in detail the atmospheric conditions observed during FD development in each season over Spain, including; large-scale atmospheric circulation patterns and synoptic situations. The main findings of this research are as follows:

1. The atmospheric dynamics underlying FDs show important seasonal differences in Spain. In winter, spring and autumn, large-scale atmospheric

circulation patterns strongly control the occurrence of FDs. Whereas in summer, when the climatology is more propitious for FD development, other thermodynamic processes may be more relevant to trigger FD conditions.

- The positive NAO is the main atmospheric driver of FDs in winter and autumn, and it is also essential in explaining FD development in spring.
- FDs are typically associated with high-pressure systems and anticyclonic situations over the Iberian Peninsula. Thus, positive and notable anomalies in Z500 and SLP were observed over western Europe and the Iberian Peninsula during the weeks prior to FD onset.
- In general, the WTs Anticyclonic Western (ANT_W_AD), East (E_AD) and Northeast (NE_AD) advection, and Anticyclonic (ANTICYC) were the most frequent during the development of FDs and also showed the highest frequency anomalies in comparison with the climatology of WTs in Spain.
- Ridge and omega blocking structures are usually frequent during FD development. In spring, ridging conditions are the main atmospheric driver of FDs.

AUTHOR CONTRIBUTIONS

Iván Noguera: Conceptualization; formal analysis; writing – review and editing; writing – original draft; data curation; visualization; investigation. **Fernando Domínguez-Castro:** Conceptualization; writing – review and editing; funding acquisition; investigation. **Sergio M. Vicente-Serrano:** Conceptualization; funding acquisition; writing – review and editing; investigation. **Ricardo García-Herrera:** Writing – review and editing; investigation. **José M. Garrido-Pérez:** Writing – review and editing; investigation. **Ricardo M. Trigo:** Writing – review and editing; investigation. **Pedro M. Sousa:** Writing – review and editing; investigation.

ACKNOWLEDGEMENTS

This work has been supported by the research projects: TED2021-129152B-C41, PID2020-116860RB-C22 and PID2022-218 137244OB-I00 financed by the Spanish Ministry of Science, Innovation and Universities.

DATA AVAILABILITY STATEMENT

The data that support the findings of this study are available from the corresponding author upon reasonable request.

ORCID


Iván Noguera  <https://orcid.org/0000-0002-0696-9504>

Fernando Domínguez-Castro  <https://orcid.org/0000-0003-3085-7040>

Sergio M. Vicente-Serrano  <https://orcid.org/0000-0003-2892-518X>

Ricardo García-Herrera  <https://orcid.org/0000-0002-3845-7458>

José M. Garrido-Pérez  <https://orcid.org/0000-0002-5071-789X>

Ricardo M. Trigo  <https://orcid.org/0000-0002-4183-9852>

Pedro M. Sousa  <https://orcid.org/0000-0002-0296-4204>

REFERENCES

- Akaike, H. (1974) A new look at the statistical model identification. *IEEE Transactions on Automatic Control*, 19(6), 716–723. Available from: <https://doi.org/10.1109/TAC.1974.1100705>
- Allen, R.G., Pereira, L.S., Raes, D. & Smith, M. (1998) Crop evapotranspiration: guidelines for computing crop water requirements. In: *FAO irrigation and drainage, paper 56*. Rome: FAO, p. 300.
- Anderson, M., Hain, C., Otkin, J., Zhan, X., Mo, K., Svoboda, M. et al. (2013) An intercomparison of drought indicators based on thermal remote sensing and NLDAS-2 simulations with U.S. drought monitor classifications. *Journal of Hydrometeorology*, 14(4), 1035–1056. Available from: <https://doi.org/10.1175/JHM-D-12-0140.1>
- Beguera, S., Vicente-Serrano, S.M., Reig, F. & Latorre, B. (2014) Standardized precipitation evapotranspiration index (SPEI) revisited: parameter fitting, evapotranspiration models, datasets and drought monitoring. *International Journal of Climatology*, 34(10), 3001–3023. Available from: <https://doi.org/10.1002/joc.3887>
- Caminero, L., Génova, M., Camarero, J.J. & Sánchez-Salguero, R. (2018) Growth responses to climate and drought at the southernmost European limit of Mediterranean *Pinus pinaster* forests. *Dendrochronologia*, 48, 20–29. Available from: <https://doi.org/10.1016/J.DENDRO.2018.01.006>
- Castro-Díez, Y., Pozo-Vázquez, D., Rodrigo, F.S. & Esteban-Parra, M.J. (2002) NAO and winter temperature variability in southern Europe. *Geophysical Research Letters*, 29(8), 1160. Available from: <https://doi.org/10.1029/2001GL014042>
- Chen, L.G., Gottschalck, J., Hartman, A., Miskus, D., Tinker, R. & Artusa, A. (2019) Flash drought characteristics based on U.S. drought monitor. *Atmosphere*, 10(9), 498. Available from: <https://doi.org/10.3390/ATMOS10090498>
- Christian, J.I., Basara, J.B., Otkin, J., Hunt, E., Wakefield, R.A., Flanagan, P.X. et al. (2019) A methodology for flash drought identification: application of flash drought frequency across the United States. *Journal of Hydrometeorology*, 20(5), 833–846. Available from: <https://doi.org/10.1175/JHM-D-18-0198.1>
- Conte, M., Giuffrida, A. & Tedesco, S. (1989) *The Mediterranean oscillation: impact on precipitation and hydrology in Italy*. Helsinki: Publications of Academy of Finland.
- Cook, B.I., Smerdon, J.E., Seager, R. & Coats, S. (2014) Global warming and 21st century drying. *Climate Dynamics*, 43(9–10), 2607–2627. Available from: <https://doi.org/10.1007/s00382-014-2075-y>
- Cortesi, N., Gonzalez-Hidalgo, J.C., Trigo, R.M. & Ramos, A.M. (2014) Weather types and spatial variability of precipitation in the Iberian Peninsula. *International Journal of Climatology*, 34(8), 2661–2677. Available from: <https://doi.org/10.1002/JOC.3866>

- Desboulets, L.D.D. (2018) A review on variable selection in regression analysis. *Econometrics*, 6(4), 45. Available from: <https://doi.org/10.3390/ECONOMETRICS6040045>
- Düinkeloh, A. & Jacobeit, J. (2003) Circulation dynamics of Mediterranean precipitation variability 1948–98. *International Journal of Climatology*, 23(15), 1843–1866. Available from: <https://doi.org/10.1002/JOC.973>
- El Kenawy, A., López-Moreno, J.I. & Vicente-Serrano, S.M. (2012) Trend and variability of surface air temperature in northeastern Spain (1920–2006): linkage to atmospheric circulation. *Atmospheric Research*, 106, 159–180. Available from: <https://doi.org/10.1016/J.ATMOSRES.2011.12.006>
- Esteban-Parra, M.J., Rodrigo, F.S. & Castro-Diez, Y. (1998) Spatial and temporal patterns of precipitation in Spain for the period 1880–1992. *International Journal of Climatology*, 18, 1557–1574. Available from: [https://doi.org/10.1002/\(SICI\)1097-0088\(19981130\)18:14](https://doi.org/10.1002/(SICI)1097-0088(19981130)18:14)
- Fernández-Montes, S., Rodrigo, F.S., Seubert, S. & Sousa, P.M. (2013) Spring and summer extreme temperatures in Iberia during last century in relation to circulation types. *Atmospheric Research*, 127, 154–177. Available from: <https://doi.org/10.1016/J.ATMOSRES.2012.07.013>
- Ford, T.W. & Labosier, C.F. (2017) Meteorological conditions associated with the onset of flash drought in the eastern United States. *Agricultural and Forest Meteorology*, 247, 414–423. Available from: <https://doi.org/10.1016/j.agrformet.2017.08.031>
- García, R., Prieto, L., Díaz, J., Hernández, E. & Del Teso, T. (2002) Synoptic conditions leading to extremely high temperatures in Madrid. *Annales Geophysicae*, 20(2), 237–245. Available from: <https://doi.org/10.5194/ANGE0-20-237-2002>
- García-Herrera, R., Díaz, J., Trigo, R.M. & Hernández, E. (2005) Extreme summer temperatures in Iberia: health impacts and associated synoptic conditions. *Annales Geophysicae*, 23(2), 239–251. Available from: <https://doi.org/10.5194/ANGE0-23-239-2005>
- García-Herrera, R., Paredes, D., Trigo, R.M., Trigo, I.F., Hernández, E., Barriopedro, D. et al. (2007) The outstanding 2004/05 drought in the Iberian Peninsula: associated atmospheric circulation. *Journal of Hydrometeorology*, 8(3), 483–498. Available from: <https://doi.org/10.1175/JHM578.1>
- García-Valero, J.A., Montavez, J.P., Jerez, S., Gómez-Navarro, J.J., Lorente-Plazas, R. & Jiménez-Guerrero, P. (2012) A seasonal study of the atmospheric dynamics over the Iberian Peninsula based on circulation types. *Theoretical and Applied Climatology*, 110(1–2), 291–310. Available from: <https://doi.org/10.1007/S00704-012-0623-0>
- Goodess, C.M. & Jones, P.D. (2002) Links between circulation and changes in the characteristics of Iberian rainfall. *International Journal of Climatology*, 22(13), 1593–1615. Available from: <https://doi.org/10.1002/JOC.810>
- Hosmer, D.W., Jovanovic, B. & Lemeshow, S. (1989) Best subsets logistic regression. *Biometrics*, 45(4), 1265–1270. Available from: <https://doi.org/10.2307/2531779>
- Hunt, E., Svoboda, M., Wardlow, B., Hubbard, K., Hayes, M. & Arkebauer, T. (2014) Monitoring the effects of rapid onset of drought on non-irrigated maize with agronomic data and climate-based drought indices. *Agricultural and Forest Meteorology*, 191, 1–11. Available from: <https://doi.org/10.1016/j.agrformet.2014.02.001>
- Ionita, M., Tallaksen, L.M., Kingston, D.G., Stagge, J.H., Laaha, G., Van Lanen, H.A.J. et al. (2017) The European 2015 drought from a climatological perspective. *Hydrology and Earth System Sciences*, 21(3), 1397–1419. Available from: <https://doi.org/10.5194/HESS-21-1397-2017>
- Jenkinson, A.F. & Collison, F.P. (1977) An initial climatology of gales over the North Sea. *Synoptic Climatology Branch Memorandum*, 62, 18.
- Jones, P.D., Jonsson, T. & Wheeler, D. (1997) Extension to the North Atlantic Oscillation using early instrumental pressure observations from Gibraltar and south-west Iceland. *International Journal of Climatology*, 17(13), 1433–1450. Available from: [https://doi.org/10.1002/\(sici\)1097-0088\(19971115\)17:13<1433::aid-joc203>3.3.co;2-g](https://doi.org/10.1002/(sici)1097-0088(19971115)17:13<1433::aid-joc203>3.3.co;2-g)
- Liang, M. & Yuan, X. (2021) Critical role of soil moisture memory in predicting the 2012 Central United States flash drought. *Frontiers in Earth Science*, 9, 615969. Available from: <https://doi.org/10.3389/FEART.2021.615969/BIBTEX>
- Lisonbee, J., Woloszyn, M. & Skumanich, M. (2021) Making sense of flash drought: definitions, indicators, and where we go from here. *Journal of Applied and Service Climatology*, 2021(1), 1–19. Available from: <https://doi.org/10.46275/JOASC.2021.02.001>
- Manzano, A., Clemente, M.A., Morata, A., Luna, M.Y., Beguería, S., Vicente-Serrano, S.M. et al. (2019) Analysis of the atmospheric circulation pattern effects over SPEI drought index in Spain. *Atmospheric Research*, 230, 104630. Available from: <https://doi.org/10.1016/J.ATMOSRES.2019.104630>
- Martín Vide, J. & Fernández, B.D. (2001) El índice NAO y la precipitación mensual en la España peninsular. *Investigaciones Geográficas*, 26, 41. Available from: <https://doi.org/10.14198/INGEO2001.26.07>
- Martin-Vide, J. & Lopez-Bustins, J.A. (2006) The Western Mediterranean Oscillation and rainfall in the Iberian Peninsula. *International Journal of Climatology*, 26(11), 1455–1475. Available from: <https://doi.org/10.1002/JOC.1388>
- Martin-Vide, J. & Olcina-Cantos, J. (2001) *Climas y tiempos de España*, Vol. 43. Madrid: Alianza Editorial.
- McEvoy, D.J., Huntington, J.L., Abatzoglou, J.T. & Edwards, L.M. (2012) An evaluation of multiscalar drought indices in Nevada and eastern California. *Earth Interactions*, 16(18), 1–18. Available from: <https://doi.org/10.1175/2012EI000447.1>
- Miró, J.R., Pepin, N., Peña, J.C. & Martin-Vide, J. (2020) Daily atmospheric circulation patterns for Catalonia (northeast Iberian Peninsula) using a modified version of Jenkinson and Collison method. *Atmospheric Research*, 231, 104674. Available from: <https://doi.org/10.1016/J.ATMOSRES.2019.104674>
- Mishra, V., Aadhar, S. & Mahto, S.S. (2021) Anthropogenic warming and intraseasonal summer monsoon variability amplify the risk of future flash droughts in India. *npj Climate and Atmospheric Science*, 4(1), 1–10. Available from: <https://doi.org/10.1038/s41612-020-00158-3>
- Mo, K.C. & Lettenmaier, D.P. (2015) Heat wave flash droughts in decline. *Geophysical Research Letters*, 42(8), 2823–2829. Available from: <https://doi.org/10.1002/2015GL064018>
- Mo, K.C. & Lettenmaier, D.P. (2016) Precipitation deficit flash droughts over the United States. *Journal of Hydrometeorology*, 17(4), 1169–1184. Available from: <https://doi.org/10.1175/JHM-D-15-0158.1>
- Molina, J. (1981) Los climas de España. Oikos-Tau, 8.

- Mukherjee, S., Mishra, A. & Trenberth, K.E. (2018) Climate change and drought: a perspective on drought indices. *Current Climate Change Reports*, 4(2), 145–163. Available from: <https://doi.org/10.1007/s40641-018-0098-x>
- Mukherjee, S. & Mishra, A.K. (2022) A multivariate flash drought indicator for identifying global hotspots and associated climate controls. *Geophysical Research Letters*, 49(2), e2021GL096804. Available from: <https://doi.org/10.1029/2021GL096804>
- Muñoz-Díaz, D. & Rodrigo, F.S. (2006) Seasonal rainfall variations in Spain (1912–2000) and their links to atmospheric circulation. *Atmospheric Research*, 81(1), 94–110. Available from: <https://doi.org/10.1016/J.ATMOSRES.2005.11.005>
- Nguyen, H., Wheeler, M.C., Otkin, J., Cowan, T., Frost, A. & Stone, R. (2019) Using the evaporative stress index to monitor flash drought in Australia. *Environmental Research Letters*, 14(6), 064016. Available from: <https://doi.org/10.1088/1748-9326/ab2103>
- Noguera, I., Domínguez-Castro, F. & Vicente-Serrano, S.M. (2020) Characteristics and trends of flash droughts in Spain, 1961–2018. *Annals of the New York Academy of Sciences*, 1472(1), 155–172. Available from: <https://doi.org/10.1111/nyas.14365>
- Noguera, I., Domínguez-Castro, F. & Vicente-Serrano, S.M. (2021) Flash drought response to precipitation and atmospheric evaporative demand in Spain. *Atmosphere*, 12(2), 165. Available from: <https://doi.org/10.3390/atmos12020165>
- Noguera, I., Vicente-Serrano, S.M. & Domínguez-Castro, F. (2022) The rise of atmospheric evaporative demand is increasing flash droughts in Spain during the warm season. *Geophysical Research Letters*, 49(11), e2021GL097703. Available from: <https://doi.org/10.1029/2021GL097703>
- Olcina-Cantos, J. (2001) Tipología de sequías en España. *Eria*, 56, 201–227. Available from: <https://doi.org/10.17811/ER.0.2001.201-227>
- Osman, M., Zaitchik, B., Badr, H., Christian, J., Tadesse, T., Otkin, J. et al. (2021) Flash drought onset over the contiguous United States: sensitivity of inventories and trends to quantitative definitions. *Hydrology and Earth System Sciences Discussions*, 25(2), 565–581. Available from: <https://doi.org/10.5194/hess-25-565-2021>
- Otkin, J., Svoboda, M., Hunt, E., Ford, T.W., Anderson, M., Hain, C. et al. (2018) Flash droughts: a review and assessment of the challenges imposed by rapid-onset droughts in the United States. *Bulletin of the American Meteorological Society*, 99(5), 911–919. Available from: <https://doi.org/10.1175/BAMS-D-17-0149.1>
- Palutikof, J. (2003) Analysis of Mediterranean climate data: measured and modelled. In: *Mediterranean climate*. Berlin-Heidelberg: Springer, pp. 125–132. Available from: https://doi.org/10.1007/978-3-642-55657-9_6
- Paredes, D., Trigo, R.M., Garcia-Herrera, R. & Trigo, I.F. (2006) Understanding precipitation changes in Iberia in early spring: weather typing and storm-tracking approaches. *Journal of Hydrometeorology*, 7(1), 101–113. Available from: <https://doi.org/10.1175/JHM472.1>
- Peña-Angulo, D., Trigo, R.M., Cortesi, N. & Gonzalez-Hidalgo, J.C. (2016) The influence of weather types on the monthly average maximum and minimum temperatures in the Iberian Peninsula. *Atmospheric Research*, 178–179, 217–230. Available from: <https://doi.org/10.1016/J.ATMOSRES.2016.03.022>
- Peña-Gallardo, M., Vicente-Serrano, S.M., Hannaford, J., Lorenzo-Lacruz, J., Svoboda, M., Domínguez-Castro, F. et al. (2019a) Complex influences of meteorological drought time-scales on hydrological droughts in natural basins of the contiguous United States. *Journal of Hydrology*, 568, 611–625. Available from: <https://doi.org/10.1016/J.JHYDROL.2018.11.026>
- Peña-Gallardo, M., Vicente-Serrano, S.M., Quiring, S., Svoboda, M., Hannaford, J., Tomas-Burguera, M. et al. (2019b) Response of crop yield to different time-scales of drought in the United States: spatio-temporal patterns and climatic and environmental drivers. *Agricultural and Forest Meteorology*, 264, 40–55. Available from: <https://doi.org/10.1016/j.agrformet.2018.09.019>
- Peng, C.Y.J., Lee, K.L. & Ingersoll, G.M. (2002) An introduction to logistic regression analysis and reporting. *Journal of Educational Research*, 96(1), 3–14. Available from: <https://doi.org/10.1080/00220670209598786>
- Potop, V., Možný, M. & Soukup, J. (2012) Drought evolution at various time scales in the lowland regions and their impact on vegetable crops in The Czech Republic. *Agricultural and Forest Meteorology*, 156, 121–133. Available from: <https://doi.org/10.1016/J.AGRFORMET.2012.01.002>
- Potopová, V., Boroneanț, C., Boincean, B. & Soukup, J. (2016) Impact of agricultural drought on main crop yields in the Republic of Moldova. *International Journal of Climatology*, 36(4), 2063–2082. Available from: <https://doi.org/10.1002/JOC.4481>
- Rodríguez-Puebla, C., Encinas, A.H., García-Casado, L.A. & Nieto, S. (2010) Trends in warm days and cold nights over the Iberian Peninsula: relationships to large-scale variables. *Climatic Change*, 100(3), 667–684. Available from: <https://doi.org/10.1007/S10584-009-9721-0>
- Rodríguez-Puebla, C., Encinas, A.H., Nieto, S. & Garmendia, J. (1998) Spatial and temporal patterns of annual precipitation variability over the Iberian Peninsula. *International Journal of Climatology*, 18(3), 299–316. Available from: [https://doi.org/10.1002/\(SICI\)1097-0088\(19980315\)18:3<299::AID-JOC247>3.0.CO;2-L](https://doi.org/10.1002/(SICI)1097-0088(19980315)18:3<299::AID-JOC247>3.0.CO;2-L)
- Rodríguez-Puebla, C., Encinas, A.H. & Sáenz, J. (2001) Winter precipitation over the Iberian peninsula and its relationship to circulation indices. *Hydrology and Earth System Sciences*, 5(2), 233–244. Available from: <https://doi.org/10.5194/HESS-5-233-2001>
- Russo, A., Gouveia, C.M., Trigo, R.M., Liberato, M.L.R. & DaCamara, C.C. (2015) The influence of circulation weather patterns at different spatial scales on drought variability in the Iberian Peninsula. *Frontiers in Environmental Science*, 3, 1. Available from: <https://doi.org/10.3389/fenvs.2015.00001>
- Sáenz, J., Rodríguez-Puebla, C., Fernández, J. & Zubillaga, J. (2001a) Interpretation of interannual winter temperature variations over southwestern Europe. *Journal of Geophysical Research Atmospheres*, 106(D18), 20641–20651. Available from: <https://doi.org/10.1029/2001JD900247>
- Sáenz, J., Zubillaga, J. & Rodríguez-Puebla, C. (2001b) Interannual winter temperature variability in the north of the Iberian Peninsula. *Climate Research*, 16(3), 169–179. Available from: <https://doi.org/10.3354/CR016169>
- Santos, J.A., Pinto, J.G. & Ulbrich, U. (2009) On the development of strong ridge episodes over the eastern North Atlantic.

- Geophysical Research Letters*, 36(17), L17804. Available from: <https://doi.org/10.1029/2009GL039086>
- Serrano, A., García, J.A., Mateos, V.L., Cancillo, M.L. & Garrido, J. (1999) Monthly modes of variation of precipitation over the Iberian Peninsula. *Journal of Climate*, 12(9), 2894–2919. Available from: [https://doi.org/10.1175/1520-0442\(1999\)012<2894:MMO VOP>2.0.CO;2](https://doi.org/10.1175/1520-0442(1999)012<2894:MMO VOP>2.0.CO;2)
- Serrano-Notivol, R., Lemus-Canovas, M., Barrao, S., Sarricolea, P., Meseguer-Ruiz, O. & Tejedor, E. (2022) Heat and cold waves in mainland Spain: origins, characteristics, and trends. *Weather and Climate Extremes*, 37, 100471. Available from: <https://doi.org/10.1016/j.wace.2022.100471>
- Serrano-Notivol, R., Tejedor, E., Sarricolea, P., Meseguer-Ruiz, O., de Luis, M., Saz, M.Á. et al. (2023) Unprecedented warmth: a look at Spain's exceptional summer of 2022. *Atmospheric Research*, 293, 106931. Available from: <https://doi.org/10.1016/J.ATMOSRES.2023.106931>
- Sousa, P.M., Barriopedro, D., García-Herrera, R., Woollings, T. & Trigo, R.M. (2021) A new combined detection algorithm for blocking and subtropical ridges. *Journal of Climate*, 34(18), 7735–7758. Available from: <https://doi.org/10.1175/JCLI-D-20-0658.1>
- Sousa, P.M., Barriopedro, D., Ramos, A.M., García-Herrera, R., Espirito-Santo, F. & Trigo, R.M. (2019) Saharan air intrusions as a relevant mechanism for Iberian heatwaves: the record breaking events of august 2018 and June 2019. *Weather and Climate Extremes*, 26, 100224. Available from: <https://doi.org/10.1016/j.wace.2019.100224>
- Sousa, P.M., Barriopedro, D., Trigo, R.M., Ramos, A.M., Nieto, R., Gimeno, L. et al. (2016) Impact of Euro-Atlantic blocking patterns in Iberia precipitation using a novel high resolution dataset. *Climate Dynamics*, 46(7), 2573–2591. Available from: <https://doi.org/10.1007/S00382-015-2718-7>
- Sousa, P.M., Trigo, R.M., Barriopedro, D., Soares, P.M.M. & Santos, J.A. (2018) European temperature responses to blocking and ridge regional patterns. *Climate Dynamics*, 50(1–2), 457–477. Available from: <https://doi.org/10.1007/S00382-017-3620-2/FIGURES/11>
- Svoboda, M., LeComte, D., Hayes, M., Heim, R.R., Gleason, K., Angel, J. et al. (2002) The drought monitor. *Bulletin of the American Meteorological Society*, 83(8), 1181–1190. Available from: [https://doi.org/10.1175/1520-0477\(2002\)083<1181:TDM>2.3.CO;2](https://doi.org/10.1175/1520-0477(2002)083<1181:TDM>2.3.CO;2)
- Tomás-Burguera, M., Castañeda, A.J., Luna, M.Y., Morata, A., Vicente-Serrano, S.M., Gonzalez-Hidalgo, J.C. et al. (2016) Control de calidad de siete variables del banco nacional de datos de AEMET. In: *X Congreso Internacional AEC: Clima, sociedad, riesgos y ordenación del territorio*. Alicante: AEC e Instituto Interuniversitario de Geografía, Universidad de Alicante, pp. 407–415.
- Tomás-Burguera, M., Vicente-Serrano, S.M., Peña-Angulo, D., Domínguez-Castro, F., Noguera, I. & El Kenawy, A. (2020) Global characterization of the varying responses of the standardized precipitation evapotranspiration index to atmospheric evaporative demand. *Journal of Geophysical Research: Atmospheres*, 125(17), e2020JD033017. Available from: <https://doi.org/10.1029/2020JD033017>
- Trigo, R.M., Añel, J., Barriopedro, D., García-Herrera, R., Gimeno, L., Nieto, R. et al. (2013) The record winter drought of 2011–12 in the Iberian Peninsula. *Bulletin of the American Meteorological Society*, 94, S41–S45.
- Trigo, R.M. & DaCamara, C.C. (2000) Circulation weather types and their influence on the precipitation regime in Portugal. *International Journal of Climatology*, 20(13), 1559–1581. Available from: [https://doi.org/10.1002/1097-0088\(200011\)20:13<1559::AID-JOC555>3.0.CO;2-5](https://doi.org/10.1002/1097-0088(200011)20:13<1559::AID-JOC555>3.0.CO;2-5)
- Trigo, R.M., Pozo-Vázquez, D., Osborn, T.J., Castro-Diez, Y., Gámiz-Fortis, S. & Esteban-Parra, M.J. (2004) North Atlantic oscillation influence on precipitation, river flow and water resources in the Iberian Peninsula. *International Journal of Climatology*, 24(8), 925–944. Available from: <https://doi.org/10.1002/JOC.1048>
- Venables, W.N. & Ripley, B.D. (2002) *Modern applied statistics with S*. New York, NY: Springer.
- Vicente-Serrano, S.M. (2021) La evolución de los estudios sobre sequías climáticas en España en las últimas décadas. *Geographical*, 73, 7–34.
- Vicente-Serrano, S.M., Beguería, S. & López-Moreno, J.I. (2010) A multiscalar drought index sensitive to global warming: the standardized precipitation evapotranspiration index. *Journal of Climate*, 23(7), 1696–1718. Available from: <https://doi.org/10.1175/2009JCLI2909.1>
- Vicente-Serrano, S.M. & Cuadrat, J.M. (2007) North Atlantic oscillation control of droughts in north-east Spain: evaluation since 1600 A.D. *Climatic Change*, 85(3–4), 357–379. Available from: <https://doi.org/10.1007/S10584-007-9285-9/METRICAL>
- Vicente-Serrano, S.M., Gouveia, C., Camarero, J.J., Beguería, S., Trigo, R., Lopez-Moreno, J.I. et al. (2013) Response of vegetation to drought time-scales across global land biomes. *Proceedings of the National Academy of Sciences*, 110(1), 52–57. Available from: <https://doi.org/10.1073/pnas.1207068110>
- Vicente-Serrano, S.M. & López-Moreno, J.I. (2005) Hydrological response to different time scales of climatological drought: an evaluation of the standardized precipitation index in a mountainous Mediterranean basin. *Hydrology and Earth System Sciences*, 9(5), 523–533. Available from: <https://doi.org/10.5194/hess-9-523-2005>
- Vicente-Serrano, S.M. & López-Moreno, J.I. (2006) The influence of atmospheric circulation at different spatial scales on winter drought variability through a semi-arid climatic gradient in Northeast Spain. *International Journal of Climatology*, 26(11), 1427–1453. Available from: <https://doi.org/10.1002/JOC.1387>
- Vicente-Serrano, S.M., López-Moreno, J.I., Lorenzo-Lacruz, J., El Kenawy, A., Azorín-Molina, C., Morán-Tejeda, E. et al. (2011) The NAO impact on droughts in the Mediterranean region. *Advances in Global Change Research*, 46, 23–40. Available from: https://doi.org/10.1007/978-94-007-1372-7_3
- Vicente-Serrano, S.M., Tomás-Burguera, M., Beguería, S., Reig, F., Latorre, B., Peña-Gallardo, M. et al. (2017) A high resolution dataset of drought indices for Spain. *Data*, 2(3), 22. Available from: <https://doi.org/10.3390/data2030022>
- Wang, L. & Yuan, X. (2018) Two types of flash drought and their connections with seasonal drought. *Advances in Atmospheric Sciences*, 35(12), 1478–1490. Available from: <https://doi.org/10.1007/S00376-018-8047-0>
- Wang, L., Yuan, X., Xie, Z., Wu, P. & Li, Y. (2016) Increasing flash droughts over China during the recent global warming hiatus.

- Scientific Reports*, 6(1), 30571. Available from: <https://doi.org/10.1038/srep30571>
- Wang, Y. & Yuan, X. (2021) Anthropogenic speeding up of South China flash droughts as exemplified by the 2019 summer-autumn transition season. *Geophysical Research Letters*, 48(9), e2020GL091901. Available from: <https://doi.org/10.1029/2020GL091901>
- Wilhite, D.A. (2000) *Drought as a natural hazard: concepts and definitions*. Lincoln: Drought Mitigation Center Faculty Publications.
- Wilhite, D.A. & Pulwarty, R.S. (2017) Drought as hazard: understanding the natural and social context. In: *Drought and water crises: integrating science, management, and policy*. Boca Raton, FL: CRC Press, pp. 3–22.
- Xoplaki, E., González-Rouco, J.F., Luterbacher, J. & Wanner, H. (2003) Mediterranean summer air temperature variability and its connection to the large-scale atmospheric circulation and SSTs. *Climate Dynamics*, 20(7–8), 723–739. Available from: <https://doi.org/10.1007/S00382-003-0304-X>
- Xu, H., Wang, X., Zhao, C. & Yang, X. (2018) Diverse responses of vegetation growth to meteorological drought across climate zones and land biomes in northern China from 1981 to 2014. *Agricultural and Forest Meteorology*, 262, 1–13. Available from: <https://doi.org/10.1016/J.AGRFORMET.2018.06.027>
- Yuan, X., Wang, L. & Wood, E.F. (2018) Anthropogenic intensification of southern African flash droughts as exemplified by the 2015/16 season. *Bulletin of the American Meteorological Society*, 99(1), S86–S90. Available from: <https://doi.org/10.1175/BAMS-D-17-0077.1>
- Yuan, X., Wang, L., Wu, P., Ji, P., Sheffield, J. & Zhang, M. (2019) Anthropogenic shift towards higher risk of flash drought over China. *Nature Communications*, 10(1), 1–8. Available from: <https://doi.org/10.1038/s41467-019-12692-7>
- Zhang, Q., Kong, D., Singh, V.P. & Shi, P. (2017a) Response of vegetation to different time-scales drought across China: spatiotemporal patterns, causes and implications. *Global and Planetary Change*, 152, 1–11. Available from: <https://doi.org/10.1016/j.gloplacha.2017.02.008>
- Zhang, Y., You, Q., Chen, C. & Li, X. (2017b) Flash droughts in a typical humid and subtropical basin: a case study in the Gan River basin, China. *Journal of Hydrology*, 551, 162–176. Available from: <https://doi.org/10.1016/j.jhydrol.2017.05.044>
- Zhang, Y., You, Q., Lin, H. & Chen, C. (2015) Analysis of dry/wet conditions in the Gan River basin, China, and their association with large-scale atmospheric circulation. *Global and Planetary Change*, 133, 309–317. Available from: <https://doi.org/10.1016/J.GLOPLACHA.2015.09.005>

SUPPORTING INFORMATION

Additional supporting information can be found online in the Supporting Information section at the end of this article.

How to cite this article: Noguera, I., Domínguez-Castro, F., Vicente-Serrano, S. M., García-Herrera, R., Garrido-Pérez, J. M., Trigo, R. M., & Sousa, P. M. (2024). Unravelling the atmospheric dynamics involved in flash drought development over Spain. *International Journal of Climatology*, 44(12), 4478–4494. <https://doi.org/10.1002/joc.8592>